A Simulating Study on Resolvable–Scale Microphysical Parameterization in a Mesoscale Model

Lin Wenshi (林文实)
Department of Atmospheric Sciences, Zhongshan University, Guangzhou 510275

Fong Soikun (冯瑞权)
Geophysical and Meteorological Observatory, Macao

Wu Chisheng (吴池胜)
Department of Atmospheric Sciences, Zhongshan University, Guangzhou 510275

Ku Chimeng (古志明)
Geophysical and Meteorological Observatory, Macao

Wang Anyu (王安宇) and Yang Yan (杨 艳)
Department of Atmospheric Sciences, Zhongshan University, Guangzhou 510275

(Received October 8, 1999; revised January 6, 2000)

ABSTRACT

The Penn State / NCAR Mesoscale Model (MM5) is used to simulate the precipitation event that occurred during 1–2 May 1994 to the south of the Yangtze River. In five experiments the Kain–Fritsch scheme is made use of for the subgrid–scale convective precipitation, but five different resolvable–scale microphysical parameterization schemes are employed. They are the simple super–saturation removal scheme, the warm rain scheme of Hsie et al. (1984), the simple ice scheme of Dudhia (1989), the complex mixed–phase scheme developed by Reisner et al. (1993), and the GSFC microphysical scheme with graupel. Our interest is how the various resolvable–scale schemes affect the domain–averaged precipitation, the precipitation distribution, the sea level pressure, the cloud water and the cloud ice.

Through a series of experiments about a warm sector rainfall case, results show that although the different resolvable–scale scheme is used, the differences of the precipitation characteristics among all five runs are not very obvious. However, the precipitation is over–predicted and the strong mesoscale low is produced by the simple super–saturation removal scheme. The warm rain scheme with the inclusion of condensation and evaporation under–predicts the precipitation and allows the cloud water to reach the 300 hPa level. The scheme of the addition of graupel increases the resolvable–scale precipitation by about 20%–30%. The inclusion of supercooled liquid water in the grid–scale scheme does not affect significantly the results.

Key words: Mesoscale model, Precipitation, Resolvable–scale microphysical parameterization

1. Introduction

The simulation of precipitation process is considered as one of the most difficult physical processes to forecast in numerical weather prediction. Over the past decades considerable effort has been made in the area of precipitation parameterization. Numerous cumulus parameterization schemes have been developed to treat the subgrid–scale convective precipitation and be incorporated into three–dimensional mesoscale models. Previous research has generally found that the results of model prediction are highly sensitive to the way that convection is treated in a mesoscale model (Kuo et al., 1997). An excellent review of the problem of cumulus parameterization for the mesoscale model is given by Molinari and Dudek (1992).

With the advance of the computing technology and with the high horizontal and vertical resolution in mesoscale models, the selection of precipitation parameterization is very important and crucial to the precipitation forecast of the case. Recent studies (Zhang, 1998; Molinari and Dudek, 1992) pointed out that the hybrid approach is the preferred choice for grid spacing from 20 to 50 km. The hybrid approach uses subgrid–scale convective parameterization (the implicit scheme) to remove the convective instability and resolvable–scale cloud microphysical parameterization of varying degrees of sophistication (the explicit scheme) to treat the cloud precipitation processes on the convective stable and nearly neutral layer.

Some inter–comparisons of a few cumulus parameterization schemes have been presented in the mesoscale numerical prediction model (Spencer and Stensrud, 1998; Wang and Seaman, 1997). The modelling studies of Kuo et al. (1996) have assessed the performance of various subgrid–scale cumulus parameterization and resolvable–scale microphysical schemes in the simulation of the explosive marine cyclogenesis. However a systematic evaluation of precipitation parameterization in the numerical prediction model is an enormous task.

This study presents an inter–comparison of a few resolvable–scale cloud microphysical parameterizations when the hybrid approach is used in a mesoscale numerical prediction model. Our objective here is to assess the performance of various resolvable microphysical schemes in the simulation of a warm–sector rainfall case. Our interest is how the various schemes affect the domain–averaged precipitation, the precipitation distribution, the sea level pressure, the cloud water and the cloud ice.

Section 2 summarizes the synoptic situation of this rainfall case. Section 3 describes the basic feature of the MM5 model used in this study and the experiment design. The simulating results of the storm and the analysis are presented in Section 4. The last section presents conlusions.

2. Overview of the event

There is a precipitation event that occurred on 1–3 May 1994 to the south of the Yangtze River and the southern China. A brief synoptic description of this case can be found in the studies by Yang (1994). At 700 hPa, 0000 UTC 30 April 1994, a ridge line was located in the south of the eastern China and the weak trough was situated on the Sichuan Basin. After 12 hours, the ridge moved eastward and a warm shear line formed over the southeast of the Yangtze River in cooperation with the western Pacific subtropical high. The shear line maintained about 36 hours in the original area, the low trough was located to the south of the Yangtze River and the ridge in the north of the East China Sea are quasi–stationary. At surface, a cold front was discovered between Hohhot and Lanzhou and a warm low in the western China at 0000 UTC 1 May. Most areas to the south of the Yangtze River and in the southern China were located behind the ridge and in front of the trough. The cold front moved slowly southeastwards and the trough extended eastward after 0000 UTC 1 May. However, the cold front was located in the northwestern Jiangxi Province as far as 1200 UTC 2 May. The rainfall event occurred from 0000 UTC 1 May to 1200 UTC 2 May to the south of the shear line at 700 hPa, that is, in the center and the north of Fujian Province, and in the center and the south of Jiangxi Province. Figure 1 presents the distribution of the observed

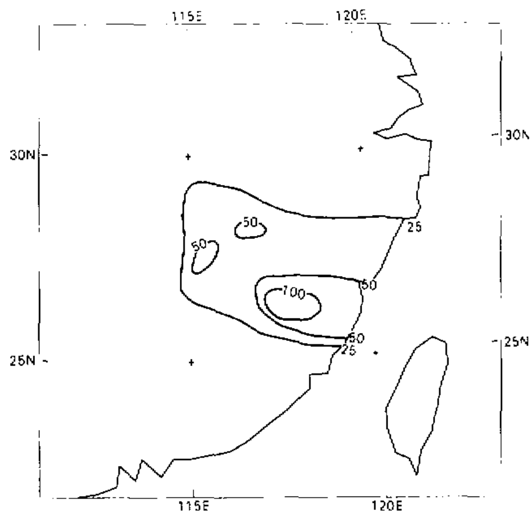

Fig. 1. The distribution of the observed 24–hour accumulated rainfall from 0000 UTC 1 May to 0000 UTC 2 May 1994.

24–hour accumulated rainfall from 0000 UTC 1 May to 0000 UTC 2 May. This event fits " warm sector rainfall" because its major rainfall occurred in the warm sector far from the cold front.

3. Model and experiment design

The Penn State / NCAR mesoscale model MM5 used in this study is a non–hydrostatic, primitive equation model with a terrain–following sigma–pressure coordinate. The planetary boundary layer (PBL) parameterization of the model includes the medium–rangeforecast (MRF) PBL schemes (Hong and Pan, 1996), asimplemented in the NCEP MRF model, which was based on the counter–gradient transport term of Troen–Mahrt representation for the unstable PBL, with vertical diffusion in the stable atmosphere and vertical mixing moist adiabatic process in clouds. The surface energy budget is used to calculate the ground temperature. 5–layer soil thermal diffusion is used to predict temperature in 1, 2, 4, 8, 16 cm layers with fixed substrate below. The long–wave and short–wave schemes (Dudhia, 1989) used for the radiation scheme with the radiation effects due to clouds are considered. The radiation is computed every 30 minutes. Detailed descriptions of the model can be found in Grell et al. (1994).

Five experiments made use of the Kain–Fritsch scheme (Kain and Fritsch 1993) for the subgrid–scale convective precipitation but employed five different resolvable–scale microphysical parameterization schemes. The first scheme (STABLE) is the simple super–saturation removal scheme. Water vapor in excess of 100% relative humidity is removed and the latent heat is added directly to the thermodynamic equation. Evaporation in unsaturated layers is not allowed. Obviously, an unrealistic treatment of cloud microphysical processes is represented in such a simple scheme. The second scheme (HSIE) is the warm rain

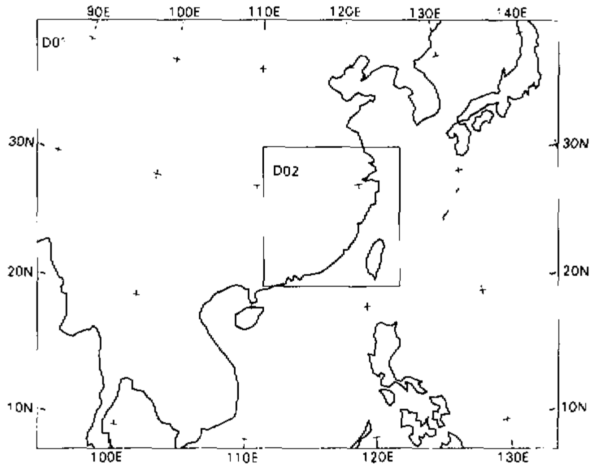

Fig. 2. Design of model domains.

scheme of Hsie et al. (1984). In this scheme, prognostic equations are included for water vapor, cloud water and rainwater. Evaporation in unsaturated layers is included. The third scheme (DUDHIA) is a simple ice scheme developed by Dudhia (1989), in which warm cloud processes are considered below and cold cloud processes above the freezing level. Instantaneous freezing and melting take place at the 0°C level. No supercooled liquid water is allowed above this level. Therefore, only a simplified treatment of the ice microphysical processes is represented in this scheme. The next scheme (REISNER) is a complex scheme developed by Reisner et al. (1993), in which five prognostic equations are used for water vapor, cloud water, rainwater, cloud ice and snow. Because the scheme allows the coexistence of liquid water and ice above the freezing level, the effects of supercooled liquid water can be included. The final scheme (GSFC) is the one developed by Tao and Simpson (1993), known as the GSFC scheme, which has six classes of water substance, including graupel. The addition of graupel allows an even more complete treatment of the precipitation processes.

The simulating experiment domain includes 2 subdomains with two–way nest (shown in Fig. 2). The grid number of the coarse domain(D01) is 75×93, its central latitude is 26°N and central longitude is 114°E, and its grid length is 54 km. The grid number of the fine domain (D02) is 73×73, and its grid length is 18 km. There are 23 sigma levels in the vertical. The full sigma levels are 1.00, 0.99, 0.98, 0.96, 0.93, 0.89, 0.85, 0.80, 0.75, 0.70, 0.65, 0.60, 0.55, 0.50, 0.45, 0.40, 0.35, 0.30, 0.25, 0.20, 0.15, 0.10, 0.05, 0.00 from surface to top. The time step is 120 seconds for the coarse domain.

The initial and boundary conditions are created through interpolating the global 2.5° resolution analyses from the National Center for Environmental Prediction (NCEP) onto the model coarse grid. After the analyzed three–dimensional fields are produced, these grid data are interpolated into the 23 model sigma levels, and the integrated mean divergence in a column is removed to reduce error growth in the model simulation.

All the experiments began at 0000 UTC 1 May 1994 and were run for 24 hours.

4. Simulation results

4.1 *Precipitation*

Figure 3a presents a time series of the simulated 4–hour domain–averaged resolvable–scale precipitation rate. The rainfall rate is computed for the areas where the amounts of 24 hours precipitation exceed about 10 mm. This figure shows that the resolvable–scale precipitation is produced in the STABLE scheme in the early period of the simulation (before 0800 UTC), while that produced by other schemes appears only in the mature and later period (from 0800 to 2400 UTC). This result indicates that the absence of microphysical process can produce excessive amounts of resolvable–scale precipitation in the forehead period of convection developing due to the unrealistic microphysical treatment in the STABLE scheme. The resolvable–scale precipitation produced by the GSFC scheme is about 20%–30% more than by the REISNER scheme after 0800 UTC. Therefore the addition of graupel in the GSFC scheme can produce more resolvable–scale precipitation. The difference between the resolvable–scale precipitation produced by the REISNER scheme and by the DUDHIA scheme is very small because the microphysical processes are basically the same in the two schemes despite the inclusion of supercooled liquid water in the REISNER scheme. Thus the inclusion of supercooled liquid water effects in the grid–scale scheme does not contribute

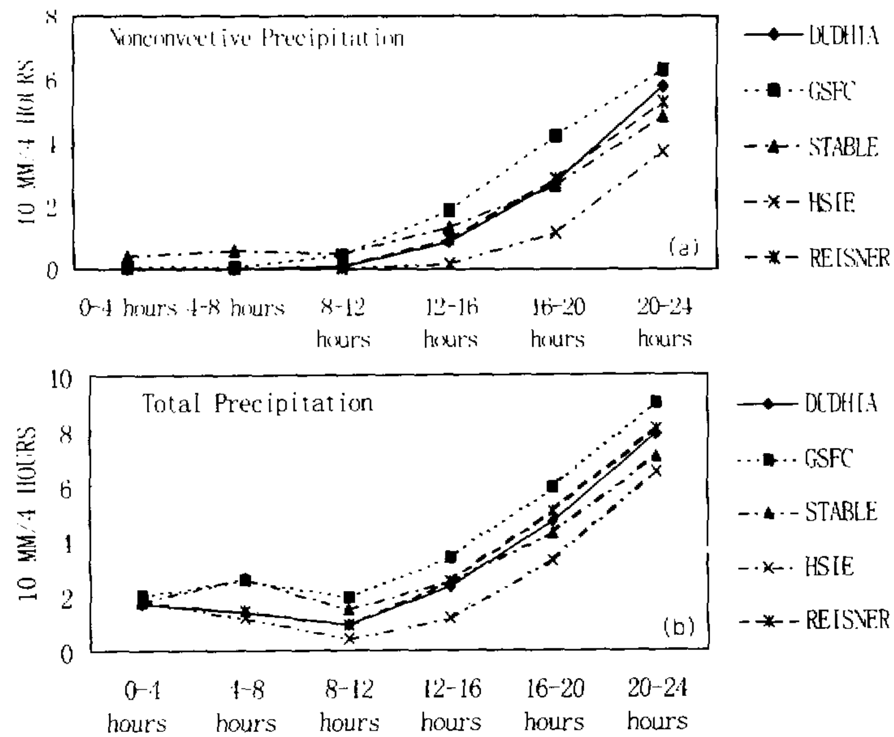

Fig. 3. Domain–averaged 4–hour precipitation rate (unit: 10 mm per 4 hours) for (a) resolvable–scale precipitation and (b) total precipitation.

significantly to the resolvable–scale precipitation. The HSIE scheme, the warm rain scheme with the inclusion of condensation and evaporation, produced resolvable–scale precipitation amounts 20%–30% less than the REISNER scheme. This suggests that the absence of the ice microphysical processes is negatively related to the resolvable–scale precipitation.

The difference among the convective precipitations with various resolvable–scale microphysical schemes is not only very small but also most of the convective precipitation rates are 10–27 mm per 4 hours (not shown). Figure 3b presents a time series of the simulated 4–hour domain–averaged accumulated precipitation rate. This figure shows that the precipitation produced by the STABLE scheme is about 15%–20% more than by the REISNER scheme before 1200 UTC because the significant resolvable–scale precipitation is produced by the STABLE scheme. The HSIE scheme produced 20%–30% less precipitation less than the REISNER scheme. The difference between the precipitation produced in the REISNER scheme and the DUDHIA scheme is also very small. However, the precipitation produced by the GSFC scheme is about 20%–30% more than other runs because it produces significant convective precipitation from 0000 to 1200 UTC and considerably large resolvable–scale precipitation from 1200 to 2400 UTC. Thus, the addition of graupel can produce more precipitation.

The percentage of the resolvable–scale precipitation in the STABLE scheme is high and that in the HSIE scheme is very low in all the period of the simulation, while that in the GSFC scheme is high in the early period of the simulation (not shown).

Figure 4 is the 24–hour simulated accumulated convective and resolvable–scale precipitation distributions in the five runs. In comparison to Fig. 1, the simulations successfully forecast the rain belt to the south of the Yangtze River. Figures 4a–4e indicate that although the different resolvable–scale schemes are used, the difference of the precipitation characteristics among all five runs is not very large: The resolvable–scale precipitation is located to the east of the convective precipitation; the difference among the convective precipitations is also not very large; the strong precipitation is mainly induced by the resolvable–scale precipitation. However, different partitioning is very apparent in resolvable–scale rain. At the same time, the different distribution of the total precipitation fields is mostly due to the development of resolvable–scale rain in the system. The strong precipitation center in the REISNER scheme and the DUDHIA scheme is the closest to the observed one although both of their positions are about 150 km north of the observation and their peak precipitation is slightly under–predicted (Fig. 4c and Fig. 4d). Interestingly, the rain areas and the maximum precipitation produced by the REISNER scheme are slightly larger than those by the DUDHIA scheme due to the inclusion of supercooled liquid water in the REISNER scheme. The HSIE scheme under–predicts the rain areas and the maximum precipitation (Fig. 4b) because of the absence of ice microphysical processes, which are smaller than that predicted by the REISNER scheme. Meanwhile, the STABLE scheme and the GSFC scheme over–predict the maximum precipitation (Fig. 4a and Fig. 4e) due to the unrealistic representation of the resolvable–scale microphysical processes or the inclusion of the graupel and both of their positions are far north of the observation.

4.2 *Sea level pressure*

Figure 5 shows the sea level pressure of the NCEP reanalysis (Fig. 5a) and the simulation at 0000 UTC 2 May. The main characteristics of the sea level pressure are successfully simulated by the five various schemes except that the 1008 hPa line of the five simulations is located westward of the observation and the pressure gradient force is over–predicted. There

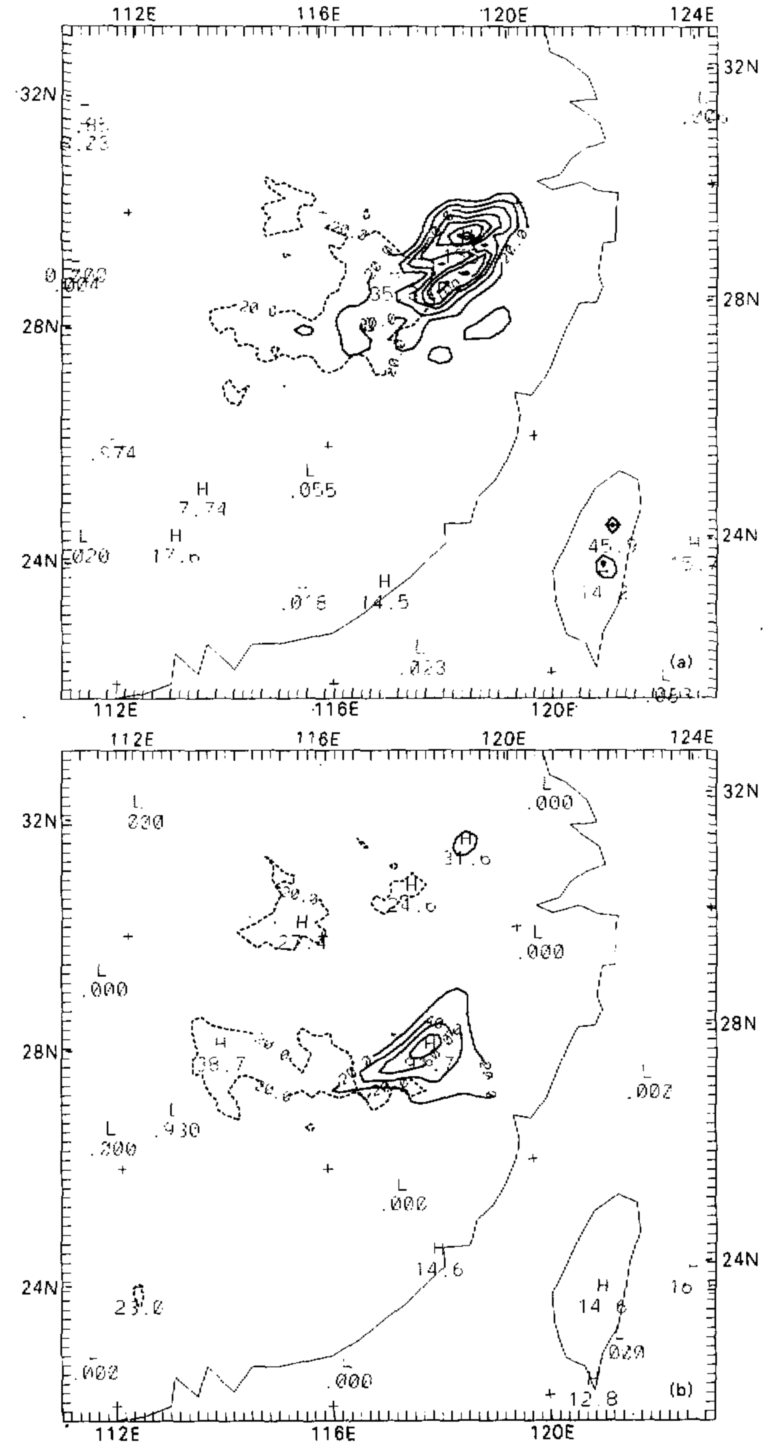
112E
116E
120E
124E
32N
28N
24N
(a)
112E
116E
120E
124E
32N
28N
24N
(b)

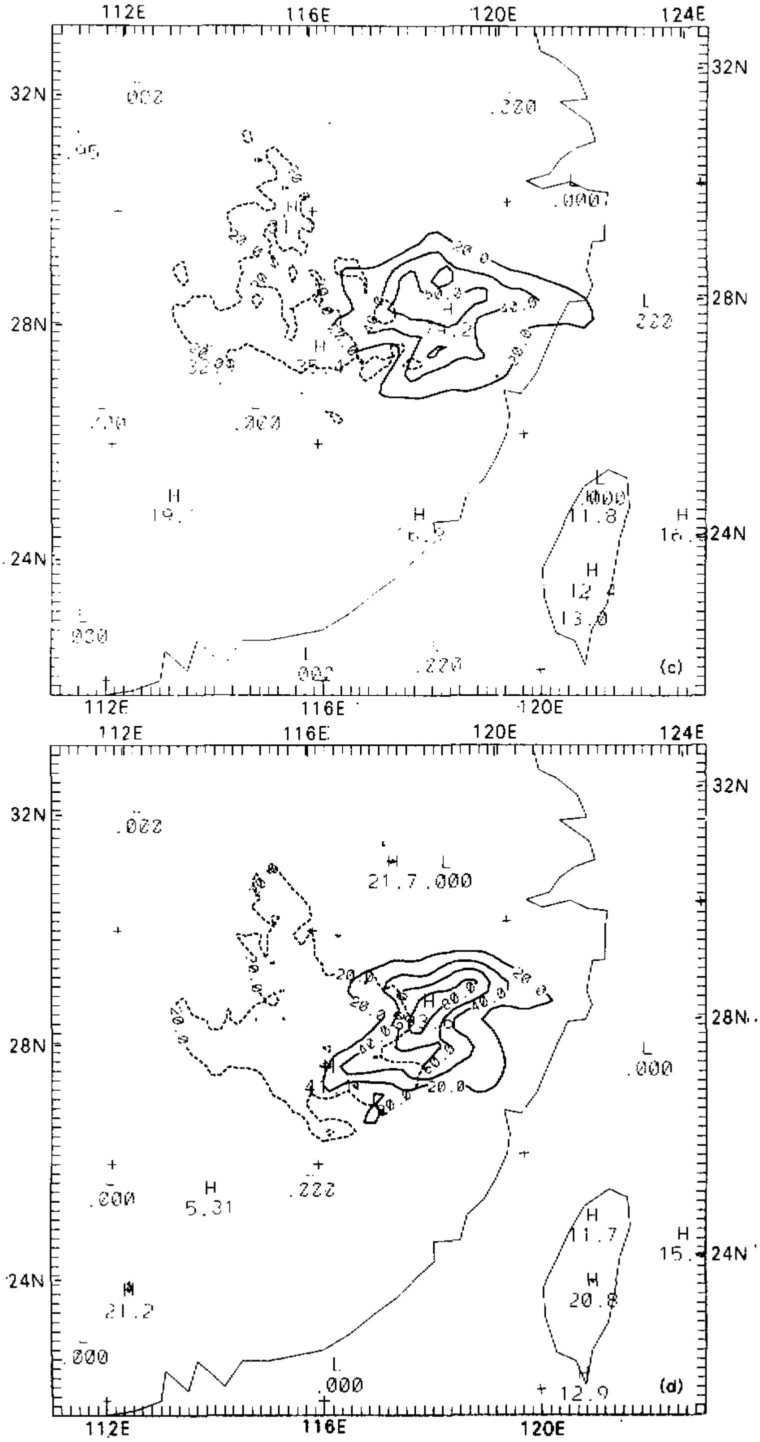
112E
116E
120E
124E
32N
28N
24N
(c)
(d)

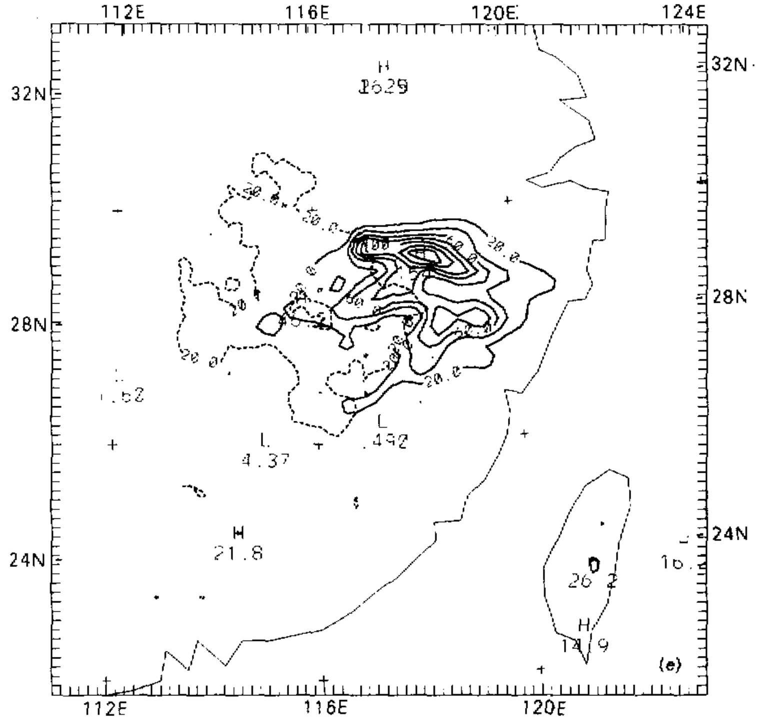

Fig. 4. Simulated 24–hour accumulated convective (solid) and resolvable–scale (dashed) precipitations (dashed) for *(a) STABLE, (b) HSIE, (c) DUDHIA, (d) REISNER, and (e) GSFC*, respectively. Contours interval is 20 mm.

are some differences among the predictions of the sea level pressure. A strong mesoscale low near 29°N is produced by the STABLE scheme (Fig. 5b). There is a deep eastward trough with three weak mesoscale lows to the south of the Yangtze River (near 28°N) by the GSFC scheme (Fig. 5f). Therefore, the resolvable–scale precipitation produced by the STABLE scheme and the GSFC scheme is over–predicted. A modest east–southeast trough near 28°N is produced by the DUDHIA scheme and by the REISNER scheme (Fig. 5d and Fig. 5e), but that by the REISNER scheme is slightly stronger than by the DUDHIA scheme. A very weak trough near 28°N is produced by the HSIE scheme, thus the resolvable–scale precipitation is under–predicted (Fig. 5c).

4.3 *Microphysical processes*

In Fig. 6, the vertical cross–sections of the cloud water content and the cloud ice content of the four various simulations at 2000 UTC 1 May 1994 have been shown respectively. It is not shown in Fig. 6 about the STABLE scheme due to no explicit cloud prediction in this scheme. Because the HSIE scheme does not consider ice phase processes and the DUDHIA scheme adds the ice phase process to the warm rain scheme without adding memory, there is no cloud ice in these two schemes. However, the cloud water can be transported to the

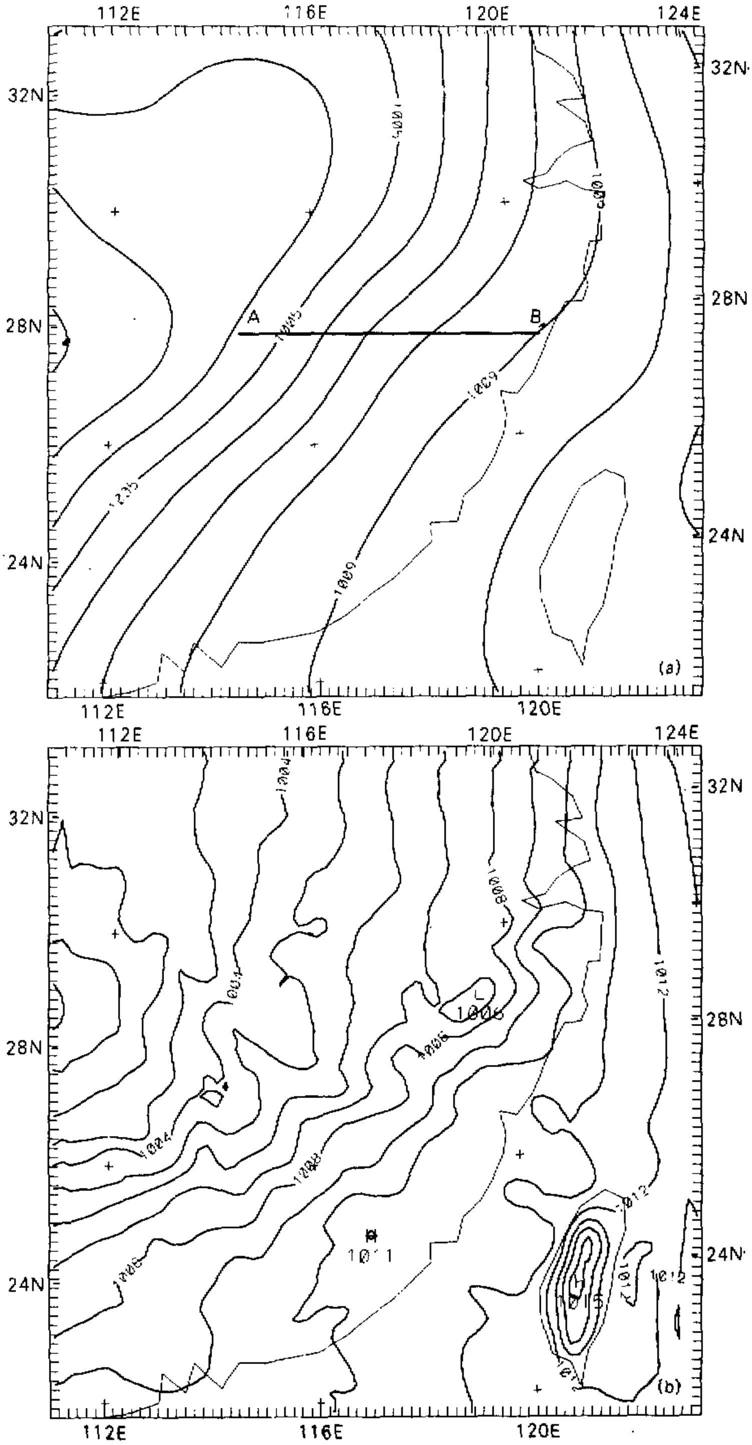
112E
116E
120E
124E
32N
28N
24N
A
B
1009
(a)
(b)
1004
1008
1006
1011
1012
1015

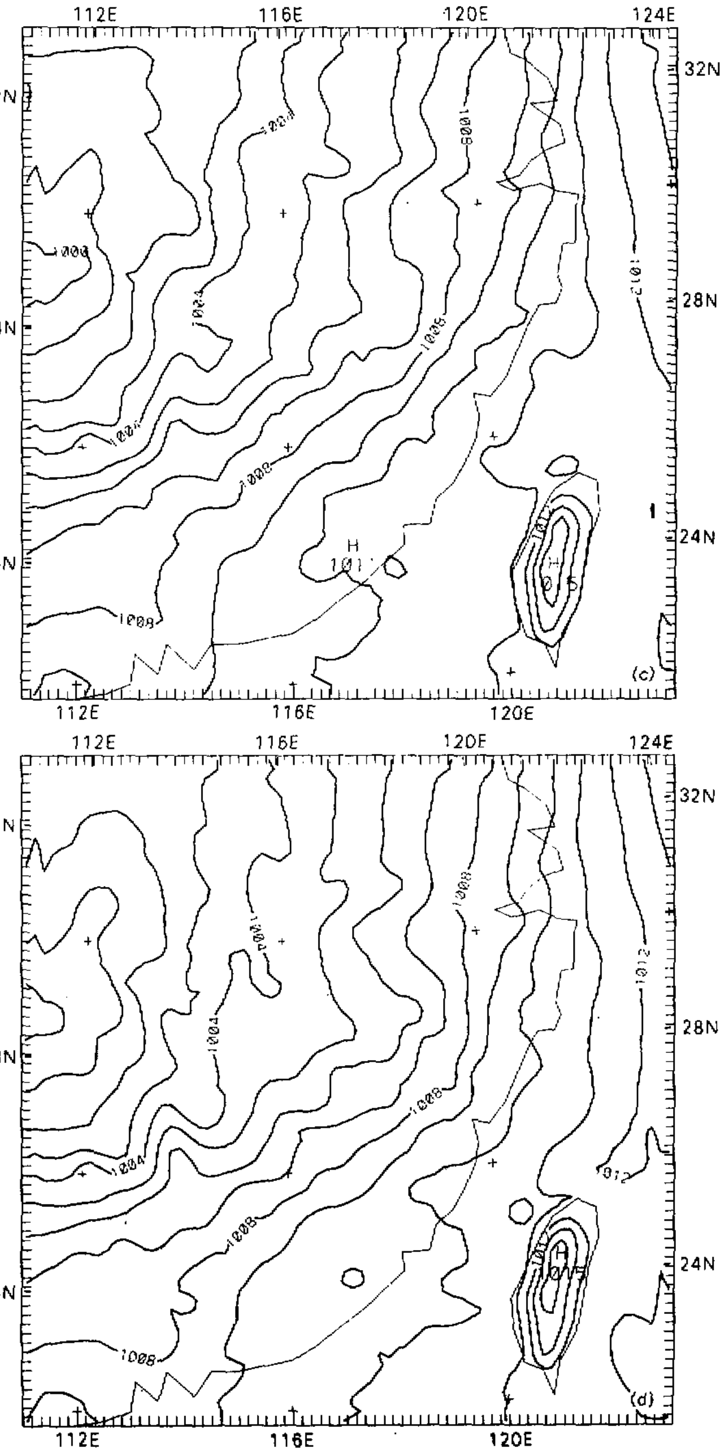
112E
116E
120E
124E
32N
28N
24N
1004
1008
1000
1012
H
(c)
(d)

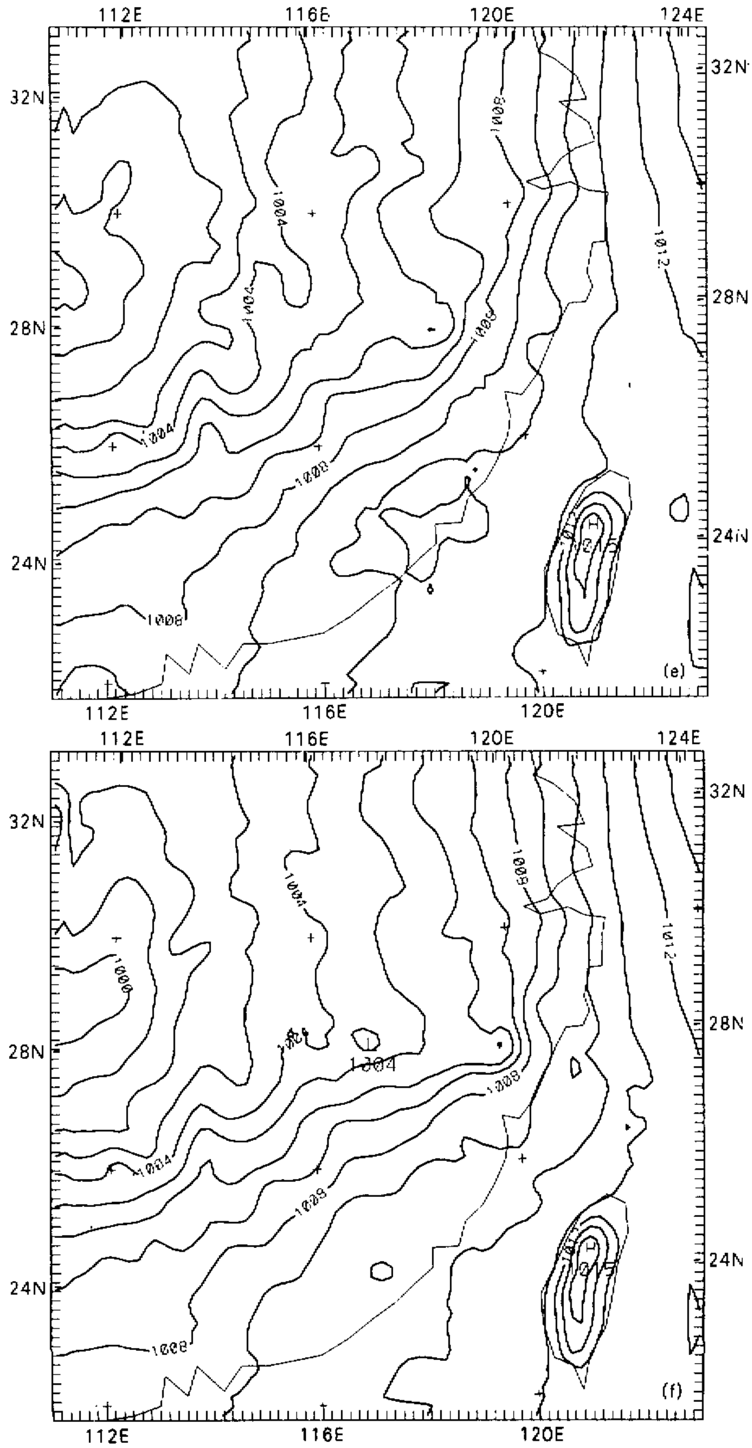

Fig. 5. Sea level pressure (hPa) of the NCEP reanalysis (a) and the simulation at 0000 UTC 2 May 1994 for (b) STABLE, (c) HSIE, (d) DUDHIA, (e) REISNER, and (f) GSFC, respectively. Contours interval is 1 hPa.

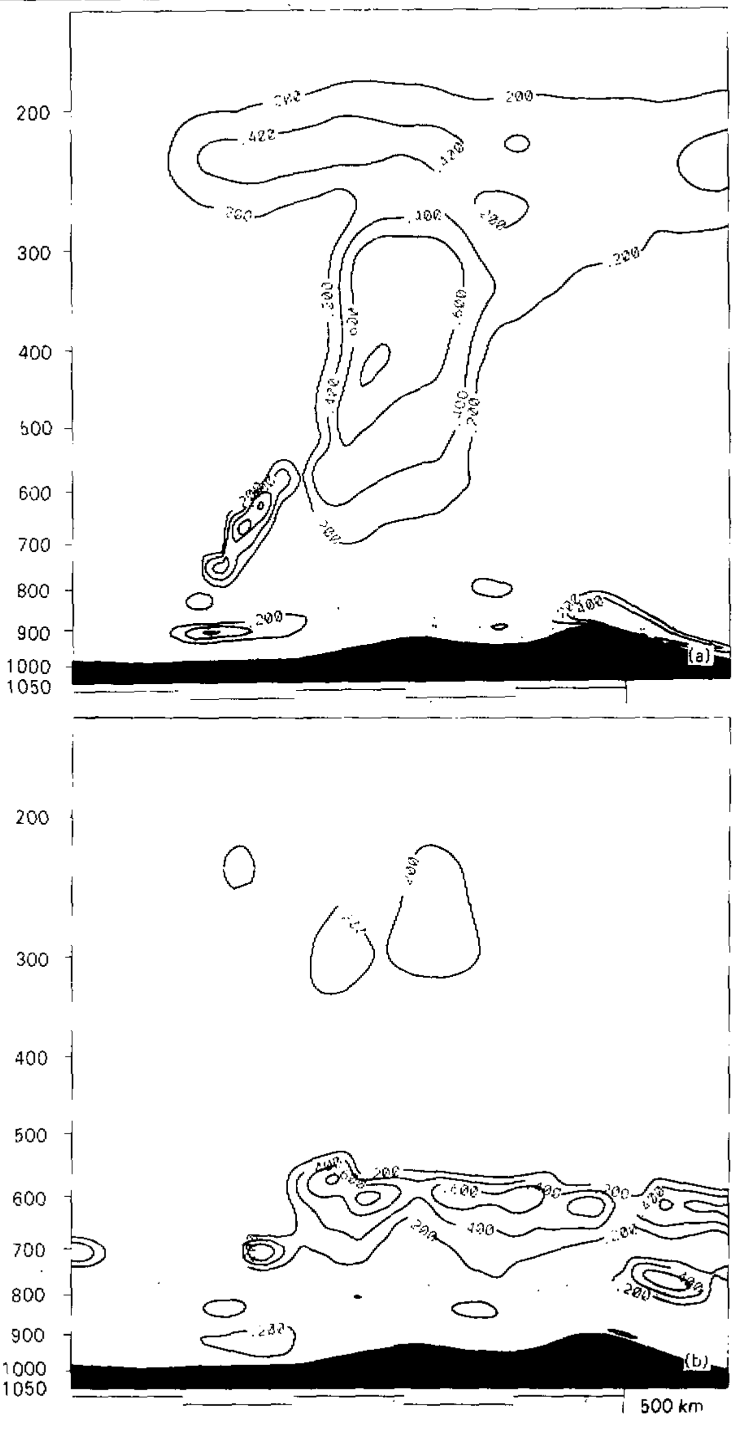
200
300
400
500
600
700
800
900
1000
1050
(a)
(b)
500 km

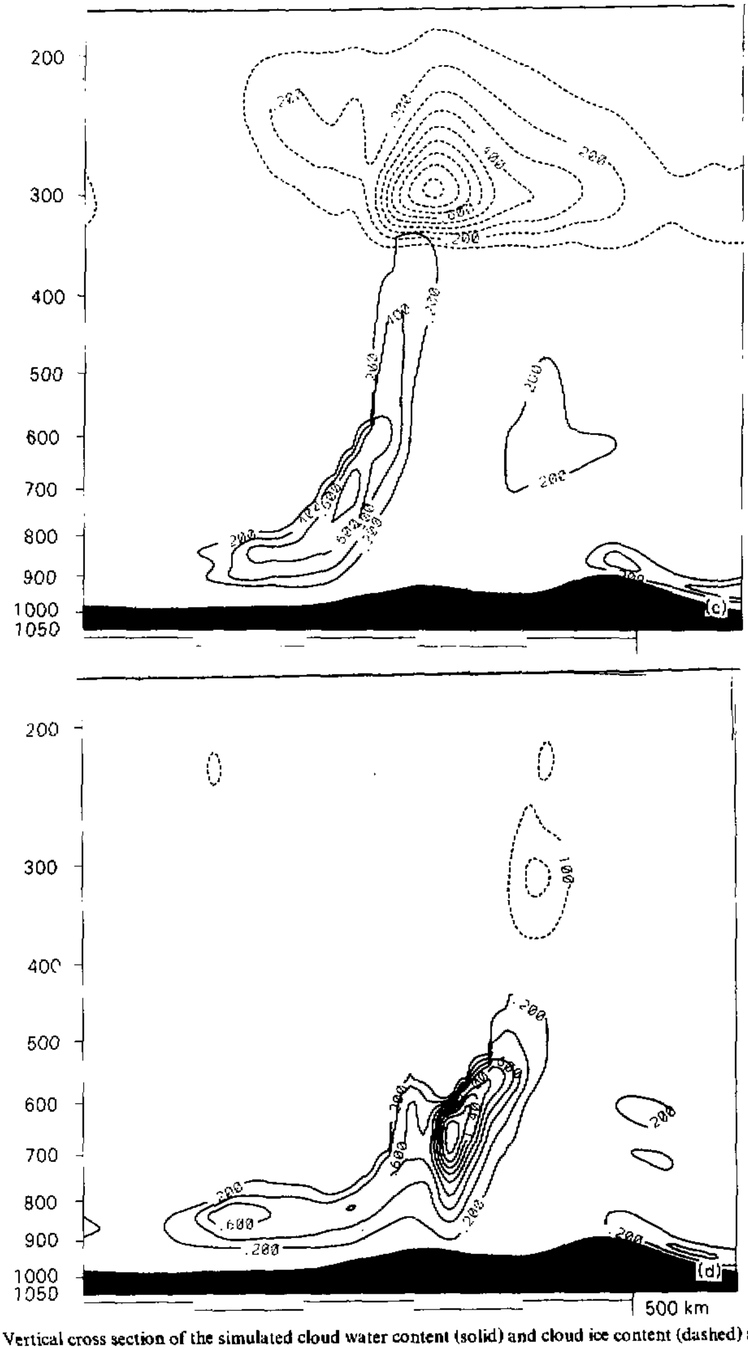

Fig. 6. Vertical cross section of the simulated cloud water content (solid) and cloud ice content (dashed) at 2000 UTC 1 May 1994, along line *AB* in Figure 5(a), for (a) HSIE, (b) DUDHIA, (c) REISNER, and (d) GSFC, respectively. Contours interval is 0.2 g / kg for solid lines and 0.1 g / kg for dashed lines.

200 hPa level due to the updraft in the HSIE scheme (Fig. 6a). The cloud water content is mainly below the 550 hPa level and largely near the 600 hPa level because instantaneous freezing and melting take place at the 0°C level in the DUDHIA scheme (Fig. 6b). There is large amount of cloud ice content above the 330 hPa level in the REISNER scheme (Fig. 6c) because its updraft velocity is high (about 1.5 m / s) at the 450 hPa level (not shown). Because the updraft velocity is low and maybe the cloud is dissipating in the GSFC scheme, the cloud ice content in this scheme is smaller than 0.25 g / kg (Fig. 6d).

5. Summary

In this paper we conducted five numerical experiments on the warm sector rainfall occurred during 1–2 May 1994 to the south of the Yangtze River using the Penn State–NCAR nonhydrostatic mesoscale model, MM5. The set of experiments utilized 2 domains with two–way nest, 54 km coarse mesh and 18 km fine mesh, with Kain–Fritsch convective parameterization and five different choices of resolvable–scale microphysical parameterization.

Through a series of experiments about the above rainfall case, some rules about different resolvable–scale microphysical processes were revealed although there were some systematic errors due to the use of the imperfect initial conditions. Tests indicated that the domain–averaged precipitation, the distribution of the total accumulated precipitation, the distribution of the resolvable–scale parameterization, and the sea level pressure were not very largely affected by the resolvable–scale schemes employed. However there are some differences among five runs, especially in microphysical characteristics due to the different treatment of microphysical processes among them. Precipitation was overpredicted and an unrealistic mesoscale low is produced if cloud microphysical processes were completely ignored. Precipitation was underpredicted if a simple warm–cloud microphysical scheme was included. Some modest improvement was made when the cold–cloud microphysical processes were included. The inclusion of the supercooled liquid water in the microphysical processes had only a minor effect on surface precipitation and sea level pressure, while the inclusion of the graupel obviously overpredicted surface precipitation and deeply affected the sea level pressure.

It needs to be pointed out that some of the conclusions are from the simulation of one case only. The results derived from this numerical study are preliminary and need to be generalized with additional case studies because the systematic inter–comparison of various precipitation parameterization schemes needs to make a great number of experiments on different cases. These cases include different scale grids, different synoptic situations, and cooperating with other physical processes. So there exists a lot of work that needs to be studied.

REFERENCES

Dudhia, J., 1989: Numerical study of convection observed during the winter monsoon experiment using a mesoscale two–dimensional model. *J. Atmos. Sci.*, **46**, 3077–3107.

Grell, G. A., J. Dudhia, and D. R. Stauffer, 1994: A description of the fifth–generation Penn State / NCAR mesoscale model (MM5), NCAR Tech Note NCAR / TN–398+STR, 138 pp.

Hong, S. Y., and H. L. Pan, 1996: Nonlocal boundary layer vertical diffusion in a medium–range forecast model. *Mon. Wea. Rev.*, **124**, 2322–2339.

Hsie, E. Y., R. A. Anthes, and D. Keyser, 1984: Numerical simulation of frontogenesis in a moist atmosphere. *J. Atmos. Sci.*, **41**, 2581–2594.

Kain, J. S., and J. M. Fritsch, 1993: Convective parameterization for mesoscale models: The Kain–Fritsch scheme. *The Representation of Cumulus in Numerical Models, Meteor. Monogr.*, No.46, Amer. Meteor. Soc., 165–177.

Kuo, Y. H., J. F. Bresch, M. D. Cheng, J. Kain, D. B. Parsons, W. K. Tao, and D. L. Zhang, 1997: Summary of a mini–workshop on cumulus parameterization for mesoscale models. *Bull. Amer. Meteor. Soc.*, **78**, 475–491.

Kuo, Y., R. J. Reed, and Y. Liu, 1996: The ERICA IOP 5 Storm. Part III: Mesoscale cyclogenesis and precipitation parameterization. *Mon. Wea. Rev.*, **124**, 1409–1434.

Molinari, J., and M. Dudek, 1992: Parameterization of convective precipitation in mesoscale numerical models: A critical review. *Mon. Wea. Rev.*, **120**, 326–344.

Reisner, J., R. T. Bruintjes, and R. J. Rasmussen, 1993: Preliminary comparisons between MM5 NCAR / Penn State model generated icing forecasts and observation. Preprints. *Fifth Intl. Conf. On Aviation Weather Systems*, Vienna, VA, Amer. Meteor. Soc., 65–69.

Spencer, P. L., and D. J. Stensrud, 1998: Simulating flash flood events: Importance of the subgrid representation of convection. *Mon. Wea. Rev.*, **126**, 2884–2912.

Tao, W. K., and J. Simpson, 1993: The GSFC cumulus ensemble mode. Part I: Model description. *Terr., Atmos. and Oceanic Sci.*, **4**, 35–72.

Wang, W., and N. L. Seaman, 1997: A comparison study of convective parameterization scheme in a mesoscale model. *Mon. Wea. Rev.*, **125**, 252–278.

Yang, G. M., 1994: The weather in May 1994. *Meteor. Mon.*, **20(8)**, 58–61 (in Chinese).

Zhang, D. L., 1998: Roles of various diabatic physical processes in mesoscale models. *Chinese Journal of Atmospheric Sciences*, **22(4)**, 548–561.